ELSEVIER

6 January 1995

Chemical Physics Letters 232 (1995) 79–89

CHEMICAL PHYSICS LETTERS

Energetics, structure and excess electrons in small sodium-chloride clusters

H. Häkkinen [1], R.N. Barnett, Uzi Landman

School of Physics, Georgia Institute of Technology, Atlanta, GA 30332, USA

Received 2 August 1994; in final form 4 November 1994

Abstract

The structure and energetics of stoichiometric $(NaCl)_n$, $1 \leqslant n \leqslant 4$, clusters, and of halide-deficient clusters in the sequence Na_4Cl_m, $0 \leqslant m \leqslant 3$, are studied using local-spin-density functional calculations, with and without exchange-correlation gradient corrections. The energy optimized structures of $(NaCl)_n$ clusters for $1 \leqslant n \leqslant 3$ are two-dimensional converting to a three-dimensional cuboid for $n=4$. The optimal structures of Na_4Cl_3 and Na_4Cl_2 are three-dimensional, deriving from that of the stoichiometric $(NaCl)_4$ parent cluster, with the excess electrons substituting for the missing halide atoms. The optimal structure of Na_4Cl is two-dimensional with the metal ions forming an approximate rhombus, and the chlorine ion capping one of the edges. In analogy with color centers in bulk ionic crystals, the excess electrons in the halogen-deficient clusters occupy energy levels which are split from the bottom of the unoccupied 'conduction band' of $(NaCl)_4$. Analysis of the electronic spatial distributions and participation ratios indicates that the excess electrons are of a more delocalized nature in comparison with the electrons occupying the p-like 'valence band'.

1. Introduction

Investigations of non-stoichiometric ionic (e.g., alkali-halide) clusters containing single or multiple excess electrons (e.g., those electrons which substitute Cl^- anions in Na_nCl_m, $0 \leqslant m < n$) open a new dimension for studies of excess-electron localization and bonding in clusters [1–14]. Particularly interesting is the 'metallization' sequence (MS) of an initially stoichiometric ionic cluster (i.e. starting from a neutral stoichiometric ionic cluster with $m=n$, and successively substituting anions by electrons, ultimately resulting in a neutral metallic cluster Na_n) which may portray a transition from an insulating to a metallic state in a finite system [2,7]. Furthermore, such non-stoichiometric ionic clusters provide finite-size analogues of bulk color centers [15], and consequently systematic investigations of such clusters allow investigations of size-evolutionary patterns of defects in condensed matter systems [2]. In this context we note that while color centers have been studied extensively in bulk crystalline alkali-halides [15], and transitions from F center to metallic behavior have been observed in bulk molten alkali halides at high excess-metal concentrations (for a review, see Ref. [16]) [17], only limited theoretical [2,6,7] and experimental [8,9,12,14] information on metal-rich alkali-halide clusters is available.

Recently [2] we have investigated Na_nF_m clusters ($1 \leqslant n \leqslant 4$, and for a given n, $0 \leqslant m < n$; and $n=14$, $0 \leqslant m \leqslant 14$), revealing certain trends of the metallization process in small clusters. These trends include: (i) structural and energetic substitutional na-

[1] Permanent address: Department of Physics, University of Jyvaskyla, 40351 Jyvaskyla, Finland.

SSDI 0009-2614(94)01327-6

ture of excess electrons in halogen-deficient alkali-halide clusters; (ii) cluster structural transitions (which can involve a change in dimensionality) upon reaching the metallization limit; (iii) electronic structure odd–even and shell-closing effects portrayed in formation energies and ionization potentials, indicating that halide-deficient clusters Na_nF_m ($m<n$) may be regarded as composed of a metallic and an ionic (alkali-halide) component, i.e. $Na_{n-m}(NaF)_m$ and (iv) layer metallization (i.e. segregation of the excess metallic component on a face of the cluster) in an intermediate-size cluster ($Na_{14}F_9$).

In our earlier investigations [2] we have used electronic structure local-spin-density functional (LSD) calculations in conjunction with classical molecular dynamics (MD) of the ions on the ground-state Born–Oppenheimer (BO) potential energy surface (a LSD-BO-MD method [18]). However in those earlier studies [2] *only the excess electrons* were considered (i.e. $n-m$ electrons in Na_nF_m, $n>m$) and their interaction with the halide anions and alkali cations were modeled by a Coulomb repulsive potential and by a local pseudo-potential, respectively. The inter-ionic interactions were described via semi-empirical parametrized potentials.

In the present calculations of sodium-chloride clusters, using the LSD-BO-MD method, we employ an accurate 'ab-initio' description of the system, by considering *all the valence electrons* in a given cluster (i.e. seven electrons for each chlorine atom and one electron for each sodium), interacting with the ions via non-local norm conserving pseudopotentials. Moreover comparative studies between spin-density functional calculations using a local approximation for the exchange–correlation functional (xc) and calculations including exchange–correlation gradient (xcg) corrections have been performed.

We focus in this Letter on stoichiometric $(NaCl)_n$, $1\leqslant n\leqslant 4$ clusters and on the metallization sequence Na_4Cl_m, $0\leqslant m\leqslant 4$ (results for other cluster sizes and corresponding metallization sequences can be found elsewhere [7]). Following a brief description of our computational method, we present our results for energetics and structure of the clusters.

2. Method

The method used in this study is based on electronic structure calculations using the local-spin-density functional Born–Oppenheimer molecular-dynamics (LSD-BO-MD) method [18], employing non-local norm-conserving pseudopotentials [19] for the valence electrons of the sodium (one electron) and chlorine (seven electrons) atoms. The nonlocal components of the pseudopotentials are treated using the Kleinman–Bylander decomposition [20], which is performed in real space [18]. Our calculations were performed on three-dimensional grids of $n_1\times n_2\times n_3$ points, with $25\leqslant n_1, n_2, n_3\leqslant 45$ depending on the cluster being investigated. We used a grid spacing of 0.7 a_0, corresponding to a kinetic-energy cutoff of the plane wave basis of $E_c=20.1$ Ry. The method is specifically suitable for studies of finite systems in various charge states and multipolar configurations [2,7,18,21–23], since it does not employ a supercell (that is a periodic replication of the ions).

In our LSD calculations we have used the local exchange–correlation functional with the Vosko–Wilks parametrization [24]. Calculations including gradient corrections, xcg (with the exchange-gradient correction of Becke [25], and the correlation-gradient correction of Perdew [26]), were performed in a post-LSD approximation; that is the gradient correction to the energy was calculated non-selfconsistently using the (self-consistent) LSD-generated electronic density [18]. As a result the geometries which we determined are optimized only at the LSD level (i.e. not including xcg corrections).

The LSD-BO-MD method can be used for structural optimization (i.e. minimization of the total energy of the system with respect to the locations of the ions using a conjugate gradient technique or via simulated annealing) and for molecular dynamics simulations [2,7,18,21–23]. In such simulations the Hellmann–Feynman forces on the ions are determined from the self-consistent solutions of the Kohn–Sham equations, which are solved, using an iterative technique, between each molecular dynamics step. Therefore, the dynamical evolution of the system is maintained on the Born–Oppenheimer potential energy surface throughout the simulation. Consequently, the length of the molecular dynamics time-step is determined by the characteristic time scale of

the classical ionic dynamics and the performance of the integration algorithm used in solving the Newtonian equations of motion. We use a fifth-order predictor–corrector algorithm with a time-step of ≈ 2–5 fs (typically, an order of magnitude larger than that used in calculations employing the fictitious Car–Parrinello Lagrangian formalism [27]). A detailed discussion of the method and its implementation for finite systems is given in Ref. [18].

3. Results

3.1. Stoichiometric clusters: $(NaCl)_n$ $(1 \leqslant n \leqslant 4)$

Experimental and theoretical studies of stoichiometric $(NaCl)_n$ alkali-halide clusters indicate that for small n the low-energy isomeric structures of these clusters consist of 'ring', 'ladder' (or 'double chain') and 'chain' motifs [28]. As the number of molecules in the cluster increases energetically optimal configurations based on the rock-salt (cubic) structural motif become prevalent. Results for the energetics of $(NaCl)_n$, $1 \leqslant n \leqslant 4$, clusters are given in Table 1 and the corresponding minimum energy structures are shown in Fig. 1.

Of the minimum energy structures shown in Fig. 1 only that of $(NaCl)_4$ is three-dimensional (3D) with a T_d symmetry, while the minimum energy structures of $(NaCl)_n$ for $n \leqslant 3$ are two-dimensional (2D), with D_{3h} and C_{2v} symmetries for the ring (R) and 'ladder' (L) isomers of $(NaCl)_3$, and a D_{2h} symmetry for the $(NaCl)_2$ cluster.

Our results, which are in good correspondence with experimental (when available) and other ab initio calculated [5,29] values, show (see Fig. 1) that in $(NaCl)_n$, $n \geqslant 2$, clusters the distances between neighboring alkali and halogen atoms, d_{Na-Cl}, are increased compared to that in the monomer molecule. Thus while in the monomer we find $d_{Na-Cl} = 2.386$ Å (compared to an experimental value of 2.361 Å [30] and 2.388 ± 0.008 Å [31]), $d_{Na-Cl} = 2.542$ Å in $(NaCl)_2$ (compared to an experimental value [31] of 2.584 ± 0.034 Å), $d_{Na-Cl} = 2.524$ Å in the R isomer of $(NaCl)_3$ (averaged over all the bonds), and $d_{Na-Cl} = 2.640$ Å in $(NaCl)_4$. We note that these values are smaller than the measured interionic distance in the bulk cubic crystal [32] where $d_{Na-Cl} = 2.814$ Å.

Inspection of the energetics of the $(NaCl)_n$,

Table 1
Energetics of stoichiometric $(NaCl)_n$ clusters

	$(NaCl)_4$	$(NaCl)_3$		$(NaCl)_2$	NaCl
		R	L		
n	4	3	3	2	1
E_T LSD	−1687.54	−1264.72	−1264.69	−842.73	−420.32
xcg	−1696.28	−1271.47	−1271.37	−847.21	−422.59
E_c	1639.33	763.80	809.22	341.44	42.25
$\Delta^{(n)}$(NaCl) LSD	2.51	1.67	1.64	2.09	-
xcg	2.22	1.67	1.57	2.03	-
$\Delta^{(n)}$(Cl) LSD	6.15	5.76	5.70	5.73	4.58
xcg	5.94	5.62	5.53	5.54	4.40
$\Delta_i^{(n)}$ LSD	29.06	20.86	20.83	13.49	5.7
xcg	28.82	20.87	20.78	13.48	5.73
$\Delta_a^{(n)}$ LSD	24.61	17.52	17.49	11.26	4.58
xcg	23.52	16.90	16.80	10.82	4.40

Total energy, E_T, core–core Coulomb energy E_c, NaCl removal energy $\Delta^{(n)}(NaCl) = E_T((NaCl)_{n-1}) + E_T(NaCl) - E_T((NaCl)_n)$, Cl removal energy $\Delta^{(n)}(Cl) = E_T(Na_nCl_{n-1}) + E(Cl) - E_T(Na_nCl_n)$, cluster dissociation energy to ions $\Delta_i^{(n)} = nE(Cl^{-1}) + nE(Na^+) - E_T((NaCl)_n)$, and cluster atomization energy $\Delta_a^{(n)} = nE(Cl) + nE(Na) - E_T(Na_nCl_n)$. For $(NaCl)_3$, R and L denote ring and ladder (double-chain) isomers, respectively. LSD denotes results obtained using local-spin-density functional calculations and xcg denotes results obtained using LSD with exchange–correlation gradient corrections. In calculations of $\Delta^{(n)}(Cl)$, $\Delta_i^{(n)}$, and $\Delta_a^{(n)}$ the following electronic energies of the atoms and their ions are used (values in parentheses refer to xcg calculations): $E(Cl) = -410.53$ eV (-412.78 eV); $E(Cl^-) = -414.62$ eV (-416.865 eV); $E(Na) = -5.205$ eV (-5.41 eV), and $E(Na^+) \equiv 0$. Energies in eV.

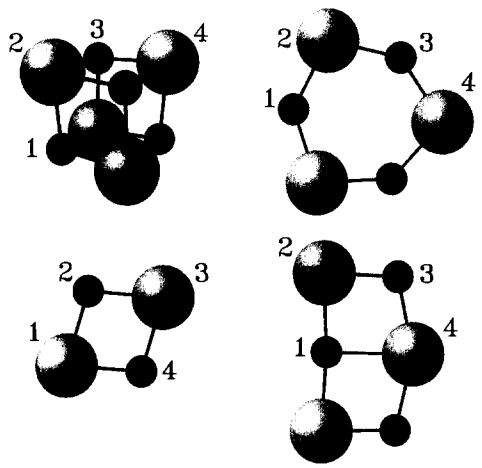

Fig. 1. Optimal geometries for $(NaCl)_n$, $2 \leqslant n \leqslant 4$, clusters, with the optimization performed at the LSD level (i.e. local exchange–correlation functional). Large and small spheres correspond to chlorine and sodium atoms, respectively. For the T_d optimal $(NaCl)_4$ cluster, $d_{Na-Cl}=2.64$ Å, $\angle(123)=82.1°$, and $\angle(234)=97.4°$ ($\angle(ijk)$ denotes the angle subtended by atoms i,j and k, with j at the apex). For the lowest-energy 2D $(NaCl_3)$ 'ring' isomer of D_{3h} symmetry, $d_{Na-Cl}=2.52$ Å, $\angle(123)=104.4°$ and $\angle(234)=135.6°$. The other 2D $(NaCl)_3$ 'ladder' isomer of C_{2v} symmetry, $d_{12}=2.58$ Å, $d_{23}=2.49$ Å, $d_{34}=2.56$ Å, $d_{14}=2.93$ Å, and $\angle(123)=85.5°$, $\angle(234)=104.4°$, $\angle(341)=77.3°$, and $\angle(412)=92.8°$. For the 2D $(NaCl)_2$ cluster of D_{2h} symmetry, $d_{12}=2.54$ Å, $\angle(123)=102.2°$, and $\angle(234)=77.8°$. In the monomer molecule NaCl $d_{Na-Cl}=2.39$ Å.

$1 \leqslant n \leqslant 4$, clusters displayed in Table 1 reveals several trends: (i) While the per-molecule Coulomb core–core repulsion energy becomes larger as n increases the total energy (electronic plus core–core Coulomb repulsion) per molecule (E_T/n, from Table 1) is approximately the same for $1 \leqslant n \leqslant 4$. (ii) The energy for removal of a halogen atom from a given cluster ($\Delta^{(n)}$(Cl) in Table 1) decreases with n, while the energy required to remove an NaCl molecule from the cluster ($\Delta^{(n)}(NaCl)=E((NaCl)_{n-1})-E((NaCl)_n)$) is smallest for $n=3$. The nonmonotonic variation of $\Delta^{(n)}$(NaCl) with n may be correlated with a change in the dimensionality of the ground-state structures; i.e. removing an NaCl molecule from $(NaCl)_4$ to form $(NaCl)_3$ (that is, $\Delta^{(4)}$(NaCl)) involves a transformation from a three-dimensional (3D) structure to a two-dimensional (2D) one, with the alkali and halide ions better coordinated in the 3D structure. The small value of $\Delta^{(3)}$(NaCl) is associated with a transformation between two 2D clusters, with the ions in the final one, $(NaCl)_2$, somewhat better coordinated than in the initial $(NaCl)_3$ cluster. (iii) The binding energy per ion-pair ($\Delta_1^{(n)}/n$, from Table 1) increases monotonically, starting from 5.73 eV for the NaCl molecule (compared to an experimental value [28] of 5.57 eV), and achieving a value of 7.205 eV for $(NaCl)_4$ which is 90% of the 'lattice energy' in a bulk [33] sodium chloride crystal (7.98 eV).

3.2. Metallization sequence: Na_4Cl_m ($0 \leqslant m < 4$)

As discussed in Section 1 the main motivations for investigations of non-stoichiometric alkali-halide clusters pertain to the nature of F centers and aggregate excess electron centers in finite systems and the systematics of insulator-to-metal transition upon metallization in a sequence of clusters [2]. Such a metallization sequence (Na_nCl_m, $0 \leqslant m \leqslant n$) starts from a stoichiometric ionic salt, Na_nCl_n (i.e. $m=n$), and ends as a metal particle, Na_n (i.e. $m=0$). As aforementioned these issues were discussed by us previously [2], using an approximate description of the electronic structure, in a study of sodium-fluoride clusters. In the following we readdress them using our current calculations for small sodium-chloride clusters.

Results pertaining to the energetics of clusters in the MS Na_4Cl_m ($1 \leqslant m < 4$) are given in Tables 2 and 3 and in Fig. 2, and structural information is shown in Figs. 3 and 4 (in Fig. 4 excess electron density contours are superimposed on the ionic structures). Excess metal non-stoichiometric alkali-halide clusters may be regarded as composed of a 'metallic' component and a molecular-ionic one, represented symbolically by $Na_nCl_m \equiv Na_{n-m}(NaCl)_m$. We note first the significant reduction in core–core repulsion upon successive removal of Cl atoms (i.e. decreasing m). Also the total energy per NaCl molecule in the cluster (i.e. E_T/m), as well as the energy for removal of a NaCl molecule from the cluster, $\Delta^{(m)}(NaCl)=E_T(Na_3Cl_{m-1})+E_T(NaCl)-E_T(Na_4Cl_m)$, decrease as m varies from $m=4$ to $m=1$. The excess-electron defect formation energy $\Delta^{(m)}$(Cl) decreases in the sequence in a non-monotonic manner, being largest for Na_4Cl_2. A similar behavior is exhibited by the ionization potentials (particularly the adiabatic ionization potential aIP, see Table 3). Such odd–even

Table 2
Energetics of nonstoichiometric Na_4Cl_m, $m \leqslant 3$

	Na_4Cl_3	Na_4Cl_2	Na_4Cl				
			A2d	B2d	3d	C2d	D2d
m	3	2	1	1	1	1	1
E_T LSD	−1270.87	−854.89	−438.59	−438.59	−438.56	−437.62	−437.69
xcg	−1277.55	−859.45	−441.27	−441.21	−441.16	−440.34	−440.40
E_c	967.09	468.22	142.70	158.05	161.02	109.60	122.79
$\Delta^{(m)}$(NaCl) LSD	2.10	1.73	1.46	1.46	1.43	0.48	0.55
xcg	1.90	1.52	1.37	1.32	1.26	0.45	0.50
$\Delta^{(m)}$(Cl) LSD	5.45	5.77	5.17	5.17	5.13	4.19	4.26
xcg	5.32	5.40	5.05	4.99	4.93	4.12	4.17
$\Delta_i^{(m)}$ LSD	21.80	15.24	8.36	8.36	8.33	7.38	7.46
xcg	21.55	14.90	8.18	8.12	8.07	7.25	7.30
$\Delta_a^{(m)}$ LSD	18.46	13.01	7.25	7.25	7.22	6.27	6.34
xcg	17.57	12.25	6.85	6.79	6.74	5.92	5.98
$\Delta_R^{(m)}$ LSD	0.008	0.03	0.08	0.08	0.05		
xcg	0.006	0.05	0.17	0.11	0.05		
$\Delta_{R,c}^{(m)}$	1.76	7.28	18.57	3.22	0.25		

Total energy E_T, core–core Coulomb energy E_c, NaCl removal energy $\Delta^{(m)}$(NaCl), Cl removal energy $\Delta^{(m)}$(Cl), dissociation energy to ions $\Delta_i^{(m)}$, and atomization energy $\Delta_a^{(m)}$. $\Delta_R^{(m)}$ is the total reorganization energy of the cluster (see text), and $\Delta_{R,c}^{(m)}$ is the part of the reorganization energy associated with only the interionic Coulomb interactions. For Na_4Cl the energies corresponding to four two-dimensional isomers (A2d, B2d, C2d and D2d) and for a three-dimensional (3d), are given. LSD denotes results obtained using local-spin-density functional calculations and xcg denotes results obtained using LSD with exchange–correlation gradient corrections. Energies in eV.

Table 3
Vertical (vIP) and adiabatic (aIP) ionization potentials, and reorganization energies $\epsilon_R = \text{vIP} - \text{aIP}$, for Na_4Cl_m, $1 \leqslant m < 4$, and for Na_n, $n \leqslant 4$, clusters

	vIP		aIP		ϵ_R	
	LSD	xcg	LSD	xcg	LSD	xcg
Na_4Cl_3	4.78	4.85	3.89	3.95	0.89	0.90
Na_4Cl_2	4.91	4.85	4.48	4.46	0.43	0.39
Na_4Cl A2d	4.66	4.80	3.92	4.10	0.74	0.70
B2d	4.36	4.49	3.92	4.05	0.44	0.44
C2d	5.26	5.39	5.17	5.31	0.09	0.08
D2d	5.25	5.39	< 3.6			
3d	4.09	4.21	3.92	4.05	0.17	0.16
Na	5.21	5.41	–	–	–	–
Na_2	5.18	5.25	5.06	5.15	0.12	0.10
Na_3	4.24	4.39	4.07	4.21	0.17	0.18
Na_4	4.35	4.37	4.33	4.36	0.02	0.01

LSD denotes results obtained using local-spin-density functional calculations and xcg denotes results obtained using LSD with exchange–correlation gradient corrections. Energies in eV.

oscillations with $(n-m)$ of $\Delta^{(n)}$(Cl) and the ionization potentials were predicted by us previously [2] in our investigations of $Na_{n-m}(NaF)_m$ metallization sequences (for $n=4$ and $n=14$), and were correlated with characteristic odd–even oscillations of energetic properties of the 'metallic' component, Na_{n-m}, of the nonstoichiometric halogen deficient clusters. While such a correlation is supported by our results

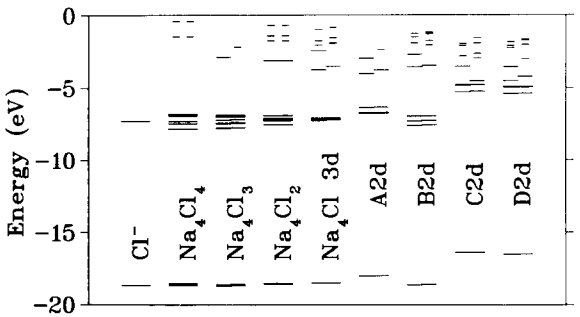

Fig. 2. LSD Kohn–Sham energy levels for Na_4Cl_m, $1 \leqslant m \leqslant 4$, clusters. For the Na_4Cl cluster, energy levels for four 2D isomers (with A2d and B2d being the optimal ones) and for a 3D isomer are shown. Also included are the KS levels for the Cl^- ion (shifted so that the s-state eigenvalue coincides with that in Na_4Cl_4). For each cluster levels for both spin orientations are shown, with up-spin on the left and down-spin on the right (when these are degenerate a long horizontal line is drawn). The shortest lines correspond to unoccupied levels and the longer ones to occupied levels.

for larger clusters [2,7], we remark that for the Na_4Cl_m ($0 \leqslant m \leqslant 4$) short metallization sequence the interpretation is complicated due to the change in the dimensionality of the optimal cluster geometries in going from Na_4Cl_2 to Na_4Cl (see below).

We also note from Table 2 that the total reorganization energy of the clusters, associated with formation of a Na_4Cl_m cluster by removal of a chlorine atom from Na_4Cl_{m+1}, is rather small; $\Delta_R^{(m)} = E_T^0(Na_4Cl_m) - E_T(Na_4Cl_m)$, where E_T^0 and E_T are the total energies of the unrelaxed (that is Na_4Cl_m in the geometry of the parent Na_4Cl_{m+1} cluster), and relaxed cluster, respectively. On the other hand the interionic Coulomb part of the cluster reorganization energy $\Delta_{R,c}^{(m)}$ (defined in analogy with $\Delta_R^{(m)}$, but using only the Coulomb energies of the clusters) is rather large. Effective cancellation between $\Delta_{R,c}^{(m)}$ and the change in the electronic energy accompanying the relaxation of the structure, results in the small calculated values for the total reorganization energies, $\Delta_R^{(m)}$. In this context we remark that the reorganization energies associated with ionization, i.e. $\epsilon_R = vIP - aIP$ (where vIP and aIP are the vertical and adiabatic ionization potentials, respectively; see Table 3), are quite significant, reflecting structural variations between the neutral and charged states of the clusters.

The electronic structure and bonding in bulk al-

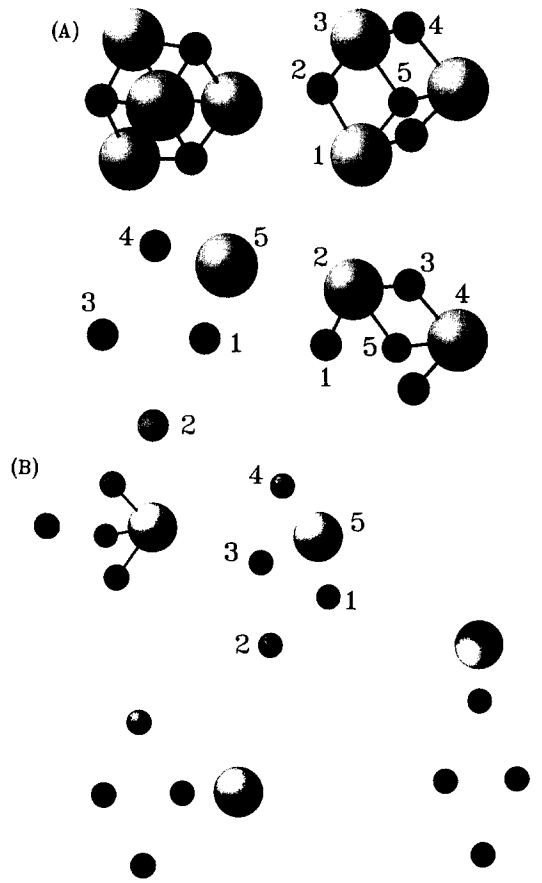

Fig. 3. (A) Optimal structures for Na_4Cl_m ($1 \leqslant m \leqslant 4$) clusters, with LSD optimization. The sequence starts with Na_4Cl_4 at the upper left corner, and going clockwise, ending with the 2D Na_4Cl (A2d) isomer shown at the lower left corner. Large and small spheres correspond to sodium and chlorine atoms, respectively. For the 3D Na_4Cl_3 cluster $d_{Na-Cl} = 2.65$ Å, $\angle(123) = 97.9°$, $\angle(234) = 83.4°$, and $\angle(235) = 81.9°$. For the 3D Na_4Cl_2 cluster $d_{12} = 2.73$ Å, $d_{23} = 2.63$ Å, $\angle(123) = 79.6°$, $\angle(234) = 103.3°$, and $\angle(345) = 76.2°$. For the Na_4Cl (A2d) $d_{12} = 3.34$ Å, $d_{23} = 3.41$ Å, $d_{34} = 3.40$ Å, $d_{14} = 3.46$ Å, $d_{15} = 2.51$ Å, $d_{45} = 2.50$ Å, $\angle(123) = 61.1°$, $\angle(234) = 119.2°$, $\angle(341) = 60.1°$, $\angle(412) = 119.6°$, and $\angle(451) = 87.5°$. (B) Optimal geometries for the 3D isomer of Na_4Cl (at the upper left corner) and, going clockwise, for the B2d, C2d and D2d isomers. For the Na_4Cl (B2d) isomer (upper right), $d_{12} = 3.20$ Å, $d_{23} = 3.47$ Å, $d_{34} = 3.34$ Å, $d_{45} = 2.60$ Å, $d_{15} = 2.57$ Å, $d_{35} = 2.69$ Å, and $\angle(354) = 78.3°$, $\angle(351) = 75.8°$, $\angle(123) = 57.9°$, $\angle(231) = 57.0°$, and $\angle(213) = 65.1°$.

kali-halide crystals are commonly classified as ionic in nature [15]. In sodium-chloride this results in cubic (rock-salt structure) crystals with a 3p-like occupied valence band (VB) separated by a wide band-

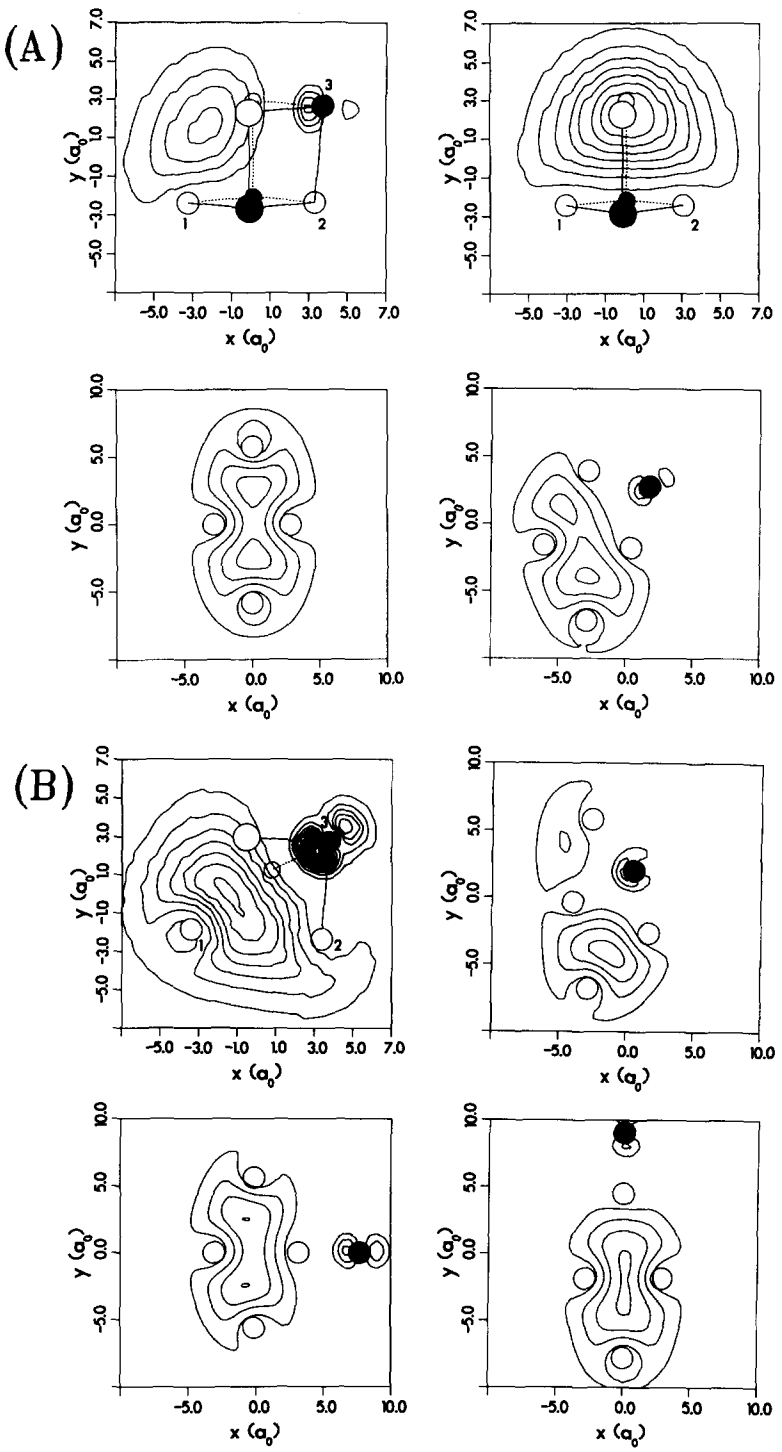

Fig. 4. (A) Contours of the excess electron(s) density (highest occupied KS orbitals, separated from the 'VB' orbitals) for the optimal structures of Na_4Cl_m ($0 \leqslant m \leqslant 3$). The figure at the upper-left corner is for Na_4Cl_3 and proceeding clockwise additional chlorine atoms are removed successively, reaching the 2D Na_4 cluster shown at the bottom left. The sodiums are denoted by open spheres and the chlorines by filled ones. The contours for Na_4Cl_3 are plotted in the plane containing atoms 1, 2 and 3; for Na_4Cl_2 in the plane containing atoms 1 and 2 and bisecting the line connecting the two chlorine atoms. For the 2D Na_4Cl (A2d) and Na_4 clusters the contours are in the plane of the atoms. (B) Same as (A) for the 3D Na_4Cl isomer (top left corner; contours in the plane contain atoms 1, 2 and 3), and, proceeding clockwise, for the B2d, C2d and D2d isomers of the cluster.

gap from an s-like unoccupied conduction band. Experimentally the band gap in sodium-chloride was determined to be $E_g = 8.6$ eV [34] and values for the VB width vary from 1.7 to 4.5 eV (the large degree of uncertainty is attributed to numerous reasons such as instrumental broadening, thermal broadening, surface charging effects, etc. [2]). The VB electronic binding energy, determined from ultraviolet photoelectron spectrometry [36], is 10.5 eV.

Inspection of the Kohn–Sham energy levels (see Fig. 2) for the metallization sequence Na_4Cl_m ($1 \leqslant m \leqslant 4$) shows that for the stoichiometric limit, $(NaCl)_4$, a p-like 'valence band' of width $w = 1.03$ eV developed with $E_g = 5.31$ eV. The VB narrows progressively upon depletion of the halide component in the MS ($w = 0.9$ eV, 0.62 eV and 0.18 eV for Na_4Cl_3, Na_4Cl_2 and Na_4Cl (3d), respectively). We note that the 3D isomer Na_4Cl (3d) is not the lowest energy configuration for this composition. Rather, the minimum-energy structures for this cluster are predicted to be two-dimensional (although the differences in total energies between the optimal 2D structures and the 3D one are small; see A2d and B2d in Table 2, see also the ionic structures shown in Figs. 3 and 4). The VB width for the A2d and B2d isomers of Na_4Cl are 0.43 eV and 0.67 eV, respectively.

The excess electrons in halide-deficient sodium-chloride clusters occupy energy levels which are split from the bottom of the unoccupied 'conduction band' (CB) of the stoichiometric $(NaCl)_4$ cluster and are located in the gap between the VB and the CB. This behavior is reminiscent of that characteristic to color centers in bulk alkali-halides [15]. The calculated gap in energy separating the top of the occupied p-like valence band from the lowest energy level associated with the excess electrons decreases gradually; i.e. 3.97, 3.77 and 3.76 eV for Na_4Cl_3, Na_4Cl_2 and Na_4Cl(3d), respectively, and 2.31 and 3.35 eV for the lowest energy isomers (A2d and B2d) of Na_4Cl (see Fig. 2).

Further characterization of the excess electrons in the halide-deficient clusters, whose spatial density distributions are shown in Fig. 4, can be given in terms of the inverse participation ratio [37], defined as

$$p_i = \int |\psi_i|^4 \, d\mathbf{r} \Big/ \left(\int |\psi_i|^2 \, d\mathbf{r} \right)^2 ,$$

where ψ_i is the ith occupied KS wavefunction, such that $p_i = 1$ for a localized state and $1/\Omega$, where Ω is the volume of the system (in our case, the volume of the wavefunctions' calculational grid), for a completely delocalized state. Comparison of the values of p_i calculated for the excess electrons (i.e. highest occupied KS levels) given in Table 4 with those corresponding to states in the 'VB' of the excess-metal clusters indicates that the excess electrons are of a more delocalized nature.

The angular momentum character of the excess electrons, obtained via a spherical-harmonics decomposition [3] of the corresponding KS eigenfunctions, is $s^{0.8}p^{0.07}d^{0.04}f^{0.03}$ for the single excess electron in Na_4Cl_3 and $s^{0.82}p^{0.05}d^{0.04}f^{0.04}$ for the two spin-paired excess electrons in Na_4Cl_2, portraying their s-like character.

The structures of the clusters in the MS are shown in Fig. 3 (for Na_4Cl_4, Na_4Cl_3, and Na_4Cl_2 only the lowest-energy structures are shown, while for Na_4Cl the lowest energy structures, denoted as A2d and B2d, as well as those of several other isomers, including a three-dimensional one, denoted as Na_4Cl(3d), are shown). In Fig. 4 we exhibit the ionic structures with superimposed contours of the excess electron(s) densities.

As seen from these figures, the minimum-energy

Table 4
Average participation ratios for the excess electron(s) wave function(s) (highest occupied KS levels), p, and for the other occupied states ('valence band'), p', for Na_4Cl_m, $m \leqslant 3$ clusters. Ω^{-1} is the inverse of the volume of the wavefunctions' calculational grid

	p	p'	Ω^{-1}
Na_4Cl_3	1.4×10^{-3}	1.0×10^{-2}	4.6×10^{-5}
Na_4Cl_2	1.2×10^{-3}	1.2×10^{-2}	4.6×10^{-5}
Na_4Cl A2d	1.2×10^{-3}	2.4×10^{-2}	1.9×10^{-5}
B2d	1.2×10^{-3}	2.4×10^{-2}	1.9×10^{-5}
3d	1.1×10^{-3}	2.4×10^{-2}	4.6×10^{-5}
Na_4	1.0×10^{-3}		1.6×10^{-5}

[2] For a compilation of experimental values and discussion see Ref. [35].

[3] The angular momentum character is calculated via analysis of the KS wavefunctions of the ith occupied state in spherical harmonics, i.e. $\psi_i(r) = \sum_{l,m} \phi^i_{lm}(r) Y_{lm}(\Omega)$ (1), with the weight of the (l, m) component given by $\omega^i_{lm} = \int [\phi^i_{lm}(r)]^2 r^2 \, dr$. In our analysis the expansion in Eq. (1) was centered about the electronic charge center of the wavefunction.

structures for Na_4Cl_3 and Na_4Cl_2 are three-dimensional, deriving from the cubic structure of the stoichiometric Na_4Cl_4 parent cluster. The excess electron(s) in these clusters are 'substitutional' in nature occupying mainly the regions of the missing halide anions (see Fig. 4A). For Na_4Cl the lowest-energy structure is two-dimensional (A2d, or the close-lying isomer B2d see also Table 2), with the single halide atom bridging an edge of the rhombus made by the four alkali atoms. The density of the excess electrons in these 2D structures of Na_4Cl is delocalized over part of the metal-atom component of the cluster (for comparison we included in Fig. 4A contours of the electron density in the Na_4 cluster).

Finally, as aforementioned two of the 2D isomers of Na_4Cl (A2d and B2d) are essentially energetically degenerate. To estimate the barrier for transition between these two isomers we have performed constrained optimization of the energy of the cluster, starting from the A2d isomer and optimizing the energy as a function of the distance d between one of the Na atoms and the Cl atom, while relaxing the positions of all the other ions in the cluster. From these calculations, the barrier height is determined to be ≈ 80 meV (see Fig. 5), indicating that at high-temperature both isomers may coexist. In this context we note that our calculations show sensitivity of the ionization potentials (particularly vIP) to the isomeric structure of the cluster, suggesting that their measurement may allow determination of the lowest-energy one.

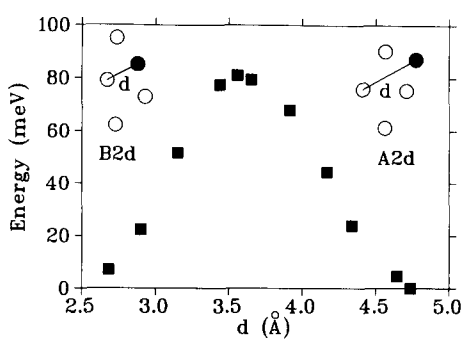

Fig. 5. Energy barrier for transformation between the A2d (right) and B2d (left) isomers of Na_4Cl, plotted as a function of the distance d between the Cl atom (filled circle) and the opposing sodium, as indicated. The data were obtained via constrained minimization. Energy in eV.

4. Summary

As a part of an extensive series of theoretical investigations [2,7] of the properties of stoichiometric and non-stoichiometric clusters of alkali-halides we studied in this Letter structural and energetic properties of $(NaCl)_n$, $1 \leqslant n \leqslant 4$ clusters, and of halide-deficient clusters Na_4Cl_m, $0 \leqslant m \leqslant 3$, comprising a metallization sequence. Our calculations employed the local-spin-density (LSD) functional method, with non-local norm-conserving pseudo-potentials and plane-wave basis sets, using a method developed for explorations of optimal structures and dynamics of finite systems on the ground-state Born–Oppenheimer potential energy surface (the LSD-BO-MD method [18]).

The optimized structures of $(NaCl)_n$ clusters for $n \geqslant 4$ are three-dimensional (3D) cuboids (rock-salt), while for $n = 2$, 3 they are two-dimensional (2D). Of the halide-deficient clusters the optimal structures are 3D for Na_4Cl_3 and Na_4Cl_2, with the ionic arrangements similar to that in the parent cubic Na_4Cl_4 cluster, and the excess electron(s) distribution is localized in the regions of the missing halide atom(s). For Na_4Cl the lowest-energy isomeric structures are 2D, with the metal ions forming an approximate rhombus (resembling the structure of Na_4) and the single chlorine ion 'capping' one of the edges of the rhombus (the two lowest isomers are practically degenerate in energy and the transformation between them involves a barrier of ≈ 80 meV). The electronic distribution of the excess electrons in these 2D clusters is of a delocalized character. Analysis of the electronic distributions and inverse participation ratios indicates that the excess electrons are of a more delocalized character than those involved in ionic bonding (the 'valence-band' electrons).

In analogy with F centers in bulk alkali-halide crystals and their aggregates (R and M centers [15]), the energy levels of the excess electrons in non-stoichiometric alkali-halide clusters are split from the bottom of the unoccupied manifold ('conduction' band) lying in the gap between the occupied ('valence band') and unoccupied levels.

These observations, together with those obtained for larger clusters (such as the metallization sequence $Na_{14}Cl_m$, $0 \leqslant m \leqslant 14$) suggest a description of non-stoichiometric alkali-halide clusters Na_nCl_m

($m<n$) as composed of 'metallic' and 'ionic' components, i.e. $Na_{n-m}(NaCl)_m$, which in sufficiently large clusters leads to structures exhibiting a face (or surface) segregated metallic layer (such as in [7] $Na_5(NaCl)_9$ or [2] $Na_5(NaF)_9$, which are composed of a segregated Na_5 layer 'adsorbed' on a face of a $3\times3\times2$ ionic crystallite). This picture is also supported by odd–even oscillation (with $n-m$) in defect formation energies (i.e. the energies for removal of successive halide atoms along the metallization sequence) and in the ionization potentials.

Acknowledgement

This research is supported by the US Department of Energy (Grant No. DE-FG05-86ER-45234). HH acknowledges partial support from the Academy of Finland. Calculations were performed on CRAY computers at the Florida State University Computing Center, the National Energy Research Supercomputer Center, Livermore, California, and the GIT Center for Computational Materials Science.

References

[1] U. Landman, D. Scharf and J. Jortner, Phys. Rev. Letters 54 (1985) 1860;
D. Scharf, U. Landman and J. Jortner, J. Chem. Phys. 87 (1987) 2716.

[2] G. Rajagopal, R.N. Barnett and U. Landman, Phys. Rev. Letters 67 (1991) 727;
U. Landman, R.N. Barnett, C.L. Cleveland and G. Rajagopal, in: Physics and chemistry of finite systems: from clusters to crystals, Vol. 1, eds. P. Jena, S.N. Khanna and B.K. Rao (Kluwer, Dordrecht, 1992) p. 165;
G. Rajagopal, Ph.D. Thesis, Georgia Institute of Technology, Atlanta (1992), and references therein.

[3] G. Galli, W. Andreoni and M.P. Tosi, Phys. Rev. A 34 (1986) 3580.

[4] G. Rajagopal, R.N. Barnett, A. Nitzan, U. Landman, E. Honea, P. Labastie, M.L. Homer and R.L. Whetten, Phys. Rev. Letters 64 (1990) 2933.

[5] P.W. Weiss, C. Ochsenfeld, R. Ahlrichs and M.M. Kappes, J. Chem. Phys. 97 (1992) 2553.

[6] V. Bonačić-Koutecký, C. Fuchs, J. Gaus, J. Pittner and J. Koutecký, Z. Physik D 26 (1993) 192.

[7] H. Häkkinen, R.N. Barnett and U. Landman, Europhys. Letters, in press; J. Phys. Chem., in press.

[8] T. Bergmann, H. Limberger and T.P. Martin, Phys. Rev. Letters 60 (1988) 1767.

[9] E.C. Honea, Ph.D. Thesis, University of California, Los Angeles (1990).

[10] E.C. Honea, M.L. Homer, P. Labastie and R.L. Whetten, Phys. Rev. Letters 63 (1989) 394;
E.C. Honea, M.L. Homer and R.L. Whetten, Phys. Rev. B 47 (1993) 7480, and references therein.

[11] S. Pollack, C.R.C. Wang and M.M. Kappes, Chem. Phys. Letters 175 (1990) 209.

[12] S. Pollack, C.R.C. Wang and M.M. Kappes, Z. Physik D 12 (1989) 241.

[13] Y.A. Yang, C.W. Conover and L.A. Bloomfield, Chem. Phys. Letters 158 (1989) 279.

[14] P. Xia and L.A. Bloomfield, Phys. Rev. Letters 70 (1993) 1779;
P. Xia, A.J. Cox and L.A. Bloomfield, Z. Physik D 26 (1993) 1841.

[15] W.B. Fowler, ed., Physics of color centers (Academic Press, New York, 1968).

[16] W.W. Warren Jr., in: The metallic and non-metallic states of matter, eds. P.P. Edwards and C.N. Rao (Taylor and Francis, London, 1985).

[17] A. Selloni, E.S. Fois, M. Parrinello and M. Car, Physica Scripta T25 (1989) 261.

[18] R.N. Barnett and U. Landman, Phys. Rev. B 48 (1993) 2081.

[19] N. Troullier and J.L. Martins, Phys. Rev. B 43 (1991) 1993.

[20] L. Kleinman and D.M. Bylander, Phys. Rev. Letters 48 (1982) 1425.

[21] R.N. Barnett and U. Landman and G. Rajagopal, Phys. Rev. Letters 67 (1991) 3058.

[22] R.N. Barnett and U. Landman, Phys. Rev. Letters 70 (1993) 1775.

[23] C. Brechignac, Ph. Cahuzac, F. Carlier, M. de Frutos, R.N. Barnett and U. Landman, Phys. Rev. Letters 72 (1994) 1636.

[24] S.H. Vosko, L. Wilks and M. Nusair, Can. J. Phys. 58 (1980) 1200;
S.H. Vosko and L. Wilks, J. Phys. C 15 (1982) 2139.

[25] A.D. Becke, Phys. Rev. A 38 (1988) 3098.

[26] J.P. Perdew, Phys. Rev. B 33 (1986) 8822; 34 (1986) 7046.

[27] R. Car and M. Parrinello, Phys. Rev. Letters 55 (1985) 2471.

[28] T.P. Martin, Phys. Rept. 95 (1983) 167.

[29] C. Ochsenfeld and R. Ahlrichs, J. Chem. Phys. 97 (1992) 3487.

[30] Y.P. Varshui and R.C. Shukla, J. Mol. Spectry. 16 (1965) 63.

[31] R.J. Mawhorter, M. Fink and J.G. Hartley, J. Chem. Phys. 83 (1985) 4418.

[32] A.F. Wells, Structural inorganic chemistry, 5th Ed. (Clarendon Press, Oxford, 1984) p. 444.

[33] J.E. Huheey, Inorganic chemistry, 3rd Ed., SI Ed. (Harper International, New York, 1983) p. 67.
[34] S. Nakai and T. Sagawa, J. Phys. Soc. Japan 26 (1969) 1427.
[35] S.C. Erwin and C.C. Lin, J. Phys. C 21 (1988) 4285 Table 1.
[36] R.T. Poole, J.G. Jenkin, J. Liesegang and R.C.G. Leckey, Phys. Rev. B 11 (1975) 5179.
[37] S.R. Elliot, Physics of amorphous materials (Longman, New York, 1984) p. 194.